Measurements of Core Radii and Peak Velocities in Modeled Atmospheric Vortices

GLENN L. BAKER AND CHRISTOPHER R. CHURCH

Department of Geosciences, Purdue University, West Lafayette, IN 47907

(Manuscript received 21 August 1978, in final form 25 July 1979)

ABSTRACT

Measurements in a tornado simulator have yielded quantitative data on certain aspects of the mean flow of a variety of modeled vortices. The radius of maximum velocity in the vortex core has been measured using a hot-film anemometer for swirl ratio values from zero to 6. A simple model of the turbulent core radius as a function of swirl ratio shows good agreement with the experimental data. The magnitude of the mean total velocity vector at the core radius has also been determined for the same range of swirl ratios and for a range of Reynolds numbers. The measurements indicate that for laminar vortices the peak velocity is strongly dependent on swirl ratio, whereas for turbulent vortices the swirl ratio dependence is weak. For both laminar and turbulent vortices, peak velocities are directly proportional to the mean vertical velocity in the updraft region. The application of the experimental measurements to the estimation of actual tornadic velocities is demonstrated.

1. Introduction

Progress in the understanding of the dynamics of tornadic vortices has long been delayed by the absence of suitable quantitative measurements of fundamental vortex features with which the results of theoretical models may be compared. Obvious features for which data are needed are the radii and maximum velocities associated with the core region. This paper presents results of an experiment to determine the response of the core radius and maximum velocity of modeled vortices to a variety of controlled dynamic and geometric parameters.

The intent in constructing the vortex simulator at Purdue University was to accurately model the dynamic and geometric character of tornadic vortex structures. Although a number of experimental chambers have been constructed in the past with similar objectives, Davies-Jones (1976) concluded that the most appropriate approach to tornado modeling is the Ward (1972) type tornado chamber. For details of the operation of the large Ward-type simulator at Purdue the reader is referred to Church *et al.* (1977, 1979).

Lewellen (1962) has shown that a complete set of governing equations in terms of the nondimensional circulation and streamfunction may be written for laminar, incompressible, axisymmetric vortex flow in a closed cylinder in terms of three nondimensional quantities: a radial Reynolds number Re_r, the swirl ratio S and a geometric aspect ratio a. These may be defined as

$$\mathrm{Re}_r = \frac{Q}{\nu}, \tag{1}$$

$$S = \frac{r_0\Gamma}{2Qh}, \tag{2}$$

$$a = \frac{h}{r_0}, \tag{3}$$

where Q is the volume flow rate per unit axial length through the chamber, ν the kinematic viscosity, r_0 the radius of the updraft region, and h the depth of the inflow layer. From an analysis of Ward's experimental data, Davies-Jones (1973) showed that the swirl ratio was the parameter which most strongly controlled the particular vortex mode observed for the experimental range of values of Re_r, S and a. Swirl ratio may also be expressed as

$$S = \frac{\tan\theta}{2a}, \tag{4}$$

where θ is the inflow angle with respect to the radial direction. Therefore, S is determined experimentally by setting the chamber dimensions to a particular aspect ratio and by measuring the inflow angle at a large radius.

It is generally recognized that intense atmospheric vortices require two dynamic ingredients: a strong convectively driven updraft and a persistent source of vorticity. The relative significance of these two quantities in producing vortices of destructive po-

0022-4928/79/122413-12$07.00

tential is, however, less well understood. To shed some light on this problem a series of measurements of the maximum vortex core velocity well away from the immediate influence of the surface boundary layer was conducted for a wide range of swirl ratios and for three values of the radial Reynolds number. The radius of maximum velocity was simultaneously obtained for each swirl ratio and flow rate condition. A simple, analytical model was developed to account for the experimental results. The implications of these results for natural tornadoes are discussed.

2. Experimental procedure

The general experimental system and procedures for obtaining mean flow measurements with hot-film sensors were substantially the same as outlined in Church *et al.* (1977). Brief mention will now be made of recent system improvements.

Vortex stability is extremely sensitive to any disturbance in the steady-state environment, and a variety of anti-turbulence screens were tried for their effectiveness in removing the large-scale turbulent elements from the inflow. A fine mesh (~0.02 mm spacing) polyester fabric which surrounds the inflow chamber was adopted. A new optically triggered pulse counting circuit provides a threefold increase in accuracy in measuring screen rotation. In normal operation the fluctuations in ring speed were measured to be less than ±0.5% of the average speed.

All chamber flow velocity measurements reported here were obtained using a hot-film anemometer sensor of length 1.0 mm and diameter 0.05 mm. Calibration curves for linearizing the sensor output were constructed for each probe over a velocity range from 0.05 to 5.0 ms^{-1}. To obtain the inflow angle measurements, the hot-film probe was azimuthally rotated in 15° increments through an angle of 90° and the resulting velocity data were then computer-fitted to the appropriate trigonometric response function.

A common means of measuring the quality of flow in wind tunnels is to report representative values of the axial relative turbulent intensity level T_r. This is defined as

$$T_r = \frac{(\overline{u'^2})^{1/2}}{U}, \tag{5}$$

where u' is the departure of the instantaneous velocity from the mean velocity U. Fig. 1 shows a typical radial scan of relative turbulent intensity in the chamber when a turbulent core vortex of swirl ratio 0.62 was being generated. This shows that the relative turbulent intensity level is less than 5%, except in the core region where, as expected, it is much higher. Because of the likelihood of flow reversal at large values of the relative turbulent intensity, turbulence values above 40% are probably underestimated.

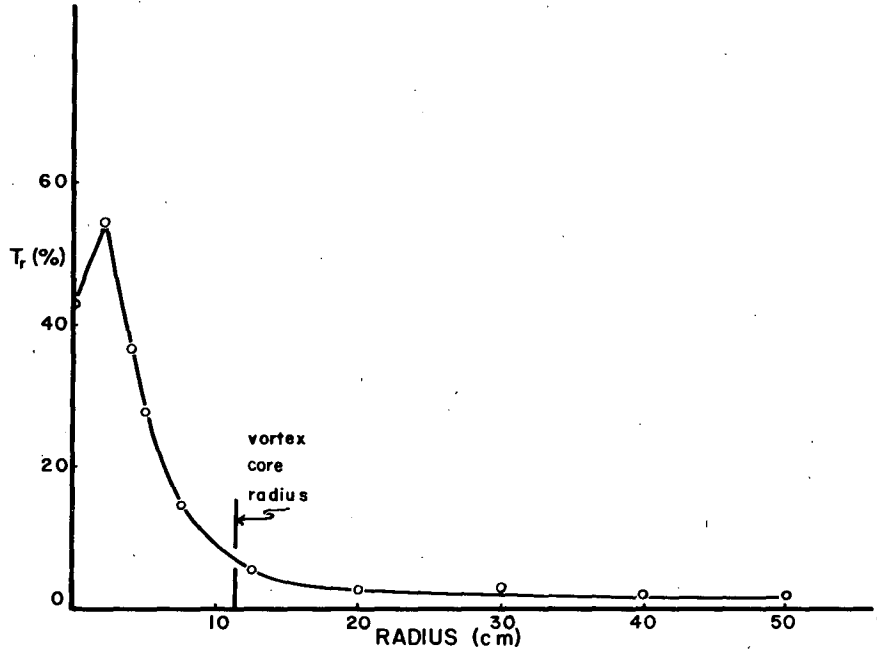

FIG. 1. The radial distribution of relative turbulent intensity in the flow field associated with a turbulent vortex core of swirl ratio 0.62. Values of T_r greater than 40% are somewhat underestimated because of limitations imposed on turbulence measurements using a single hot-film sensor.

In his experiment, Ward measured the inflow angle using a sensitive wind vane and estimated core radii from observations of the smoke-filled cores of turbulent vortices. Preliminary efforts by the authors to duplicate this technique proved to be unreliable and in the present experiment these quantities were measured using a hot-film sensor. Ward's experimental conditions were duplicated as far as possible. The inflow depth and updraft radius were kept constant at 40 and 60 cm, respectively, giving an aspect ratio of 0.67. Three series of measurements were done, one at a volume flow rate of 0.402 $m^3 s^{-1}$, one at 0.665 $m^3 s^{-1}$ and one at 1.06 $m^3 s^{-1}$ over a range of swirl ratios from zero to 6. This represents a considerable extension of the core radius measurements made by Ward and encompasses the most likely range for atmospheric vortices as estimated by Church (1979). The hot-film sensor was placed at a height of 20 cm with its axis aligned in the radial direction. The radius of maximum velocity was determined by sampling the velocity at a number of different radial positions. In general, the hot-film output contained large turbulent fluctuations, and, in order to obtain a representative mean value at each point, the output signal was filtered. Before each reading was taken the output was displayed for several minutes on a storage oscilloscope. The standard error in the absolute values of velocity was estimated as 9%. This figure comes from an extensive error analysis of the tornado chamber measurement procedure. The core radius could be determined to an accuracy of ±0.5 cm. Measurements were made on vortices with core radii up to 40 cm. The swirl ratio was measured by determining the inflow angle θ at a radius of 80 cm and at a height of 20 cm and by then applying Eq. (4). The standard error in θ was estimated as typically 2°.

3. Results

a. The core radius

Fig. 2 shows the resulting values of nondimensional core radius plotted against the swirl ratio S. For purposes of comparison, Ward's results are also included in this figure. It can be seen from examination of the two sets of results that the present data lie below Ward's data, i.e., for a given value of swirl ratio, the core radius measured in the Purdue simulator was about half that measured in Ward's machine.

The experimental data show the core radius to be a monotonically increasing function of the swirl ratio, over the full range of swirl ratio values measured. For small values of S ($\lesssim 0.8$) the data show a slight positive curvature before changing to a uniformly negative curvature above $S = 0.8$. Although the nondimensional core radius appears to be approaching a value of unity at large S it is not immediately obvious from the data what the asymptotic value is.

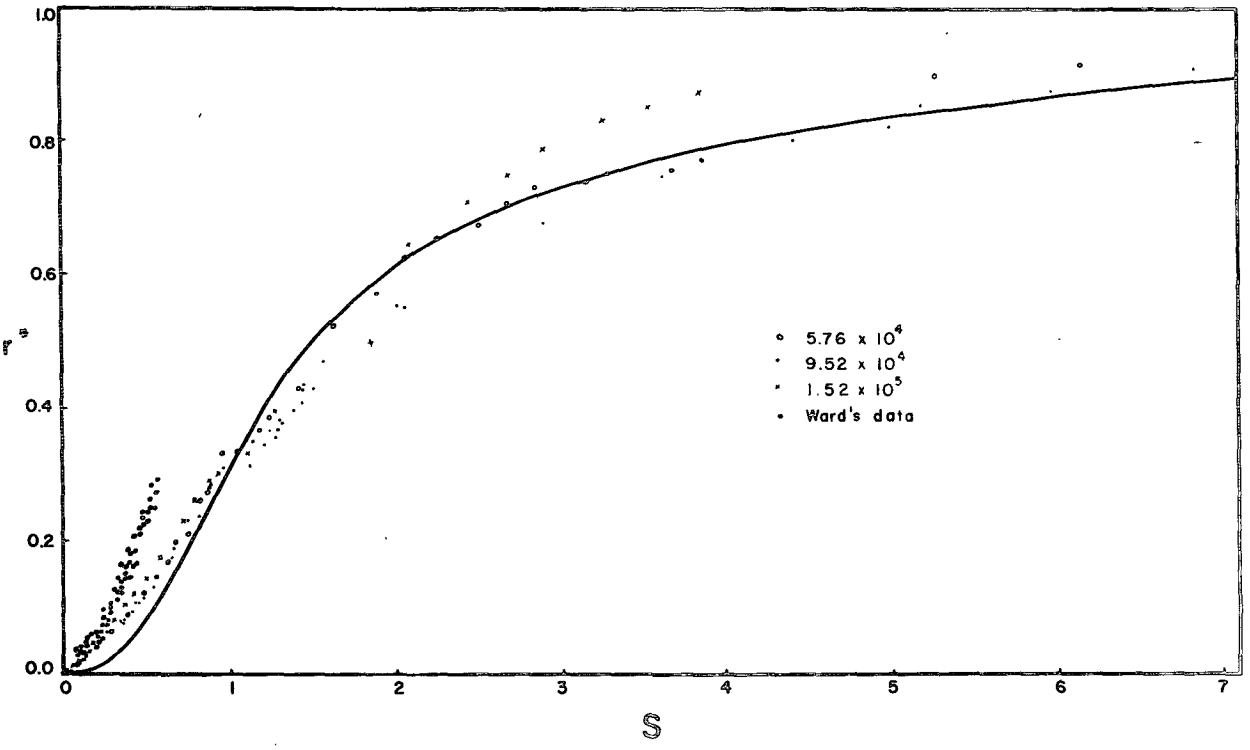

FIG. 2. Results of the nondimensional core radius ($r^* = r_1/r_0$) plotted against the swirl ratio S. Data for three values of radial Reynolds number are shown together with Ward's data (solid dots). The smooth curve is from the theoretical analysis of Section 4.

b. The maximum core velocity

The results of the measurements of the maximum mean total velocity in the core wall are shown in Fig. 3. The velocity data have been nondimensionalized by the mean vertical velocity $\bar{w}$ through the horizontal plane $z = h$ defined by $Qh = \pi r_0^2 \bar{w}$. Several features may be noted with regard to this figure:

1) The maximum mean velocity vector $|\mathbf{V}_m|/\bar{w}$ remains nearly constant through a wide range of meteorologically important swirl ratio values at a nondimensional value of ~2.6.

2) Above $S \approx 2$, $|\mathbf{V}_m|/\bar{w}$ increases in a nearly linear fashion for all three flow rates. (The differences in the rates of increase for the different flow rates is probably due to the particular method used to determine the swirl ratio which introduced an unavoidable systematic error for each flow rate experiment. It is felt by the authors that these data would also lie close to a single curve if more accurate values of S could be secured.)

3) For values of S between 0 and 0.4, $|\mathbf{V}_m|/\bar{w}$ increases very rapidly from ~0.4 to 2.6.

4) Tentative identification of certain features in the $|\mathbf{V}_m|/\bar{w}$ curves with characteristic vortex modes have been made. The rapidly rising portion of the data for S values between zero and ~0.4 corresponds to a smooth, laminar vortex structure (Church *et al.*, 1979). The slight peak in the curves near $S = 0.5$ appears to be associated with the transition from a laminar to a turbulent vortex. The second peak is apparently associated with a well-developed double vortex structure. The particular S value identified for each of these vortex structures is dependent on the radial Reynolds number and is consistent with the variation of the critical transition swirl ratio with the radial Reynolds number noted in Church *et al.* (1979).

5) The maximum velocity is very nearly linearly proportional to the radial Reynolds number Q/ν. This is shown by the fact that the results for the three Reynolds numbers may be conveniently col-

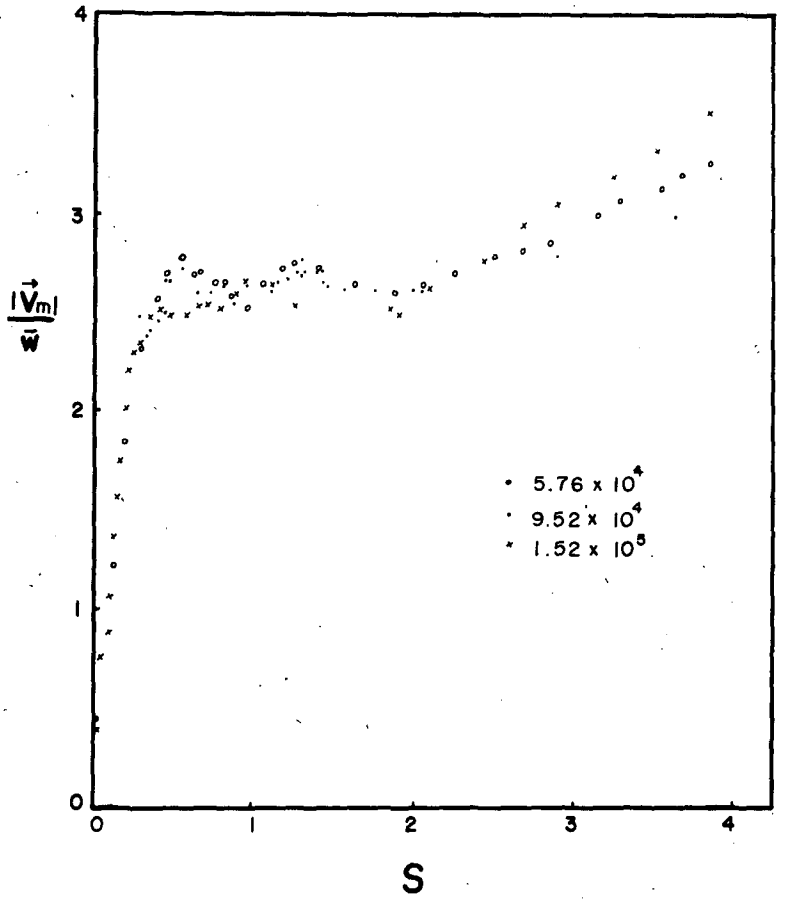

FIG. 3. Measurements of the mean total core velocity $|\mathbf{V}_m|$ nondimensionalized by the mean updraft velocity at the top of the inflow layer. Data for three radial Reynolds numbers are shown.

lapsed into a single curve, when the maximum velocity is normalized by $\bar{w}$.

c. *Vertical structure of the core*

The core radius and peak velocity measurements presented in Figs. 2 and 3 were all made at one horizontal level well away from the surface. A further experiment was conducted to determine how the core radius and peak velocity varied with axial position, as a result of the influence of the lower surface boundary layer. These two quantities were measured in a turbulent, two-celled vortex at $S = 0.97$ and $\mathrm{Re}_r = 4.82 \times 10^4$. Measurements were made from the top of the inflow layer to within 1 cm of the lower surface. The results are shown in Fig. 4. The magnitude of the total velocity vector remains fairly constant from 10 to 30 cm at a value of ~0.75 m s^{-1}. Below 10 cm the velocity increases to a maximum value of about 0.96 m s^{-1} at 3 cm (an increase of 28%) before dropping rapidly near the surface. The core radius responds in a complementary manner. The radius from 13 to 30 cm is ~21.5 cm. Below this level the core expands to ~23 cm before decreasing steadily to 12 cm at 1 cm above the surface. Thus the results shown in Fig. 4 demonstrate that the core radius and peak velocity measurements are truly representative of the downstream flow in the erect turbulent column well away from the surface.

4. Analysis

a. *The core radius*

An analytical determination of the full-scale tornadic vortex core radius is made difficult by the uncertainty associated with the choice of downstream boundary conditions. Until a more refined picture of the structure of severe storms is obtained, any choice of those boundary conditions must remain highly speculative. On the other hand, the downstream boundary conditions in the Ward-type tornado simulator are well known. A simple analysis of the radius of the turbulent vortex core based on these boundary conditions is presented here as an initial step toward a more complete understanding of the very formidable full-scale phenomenon.

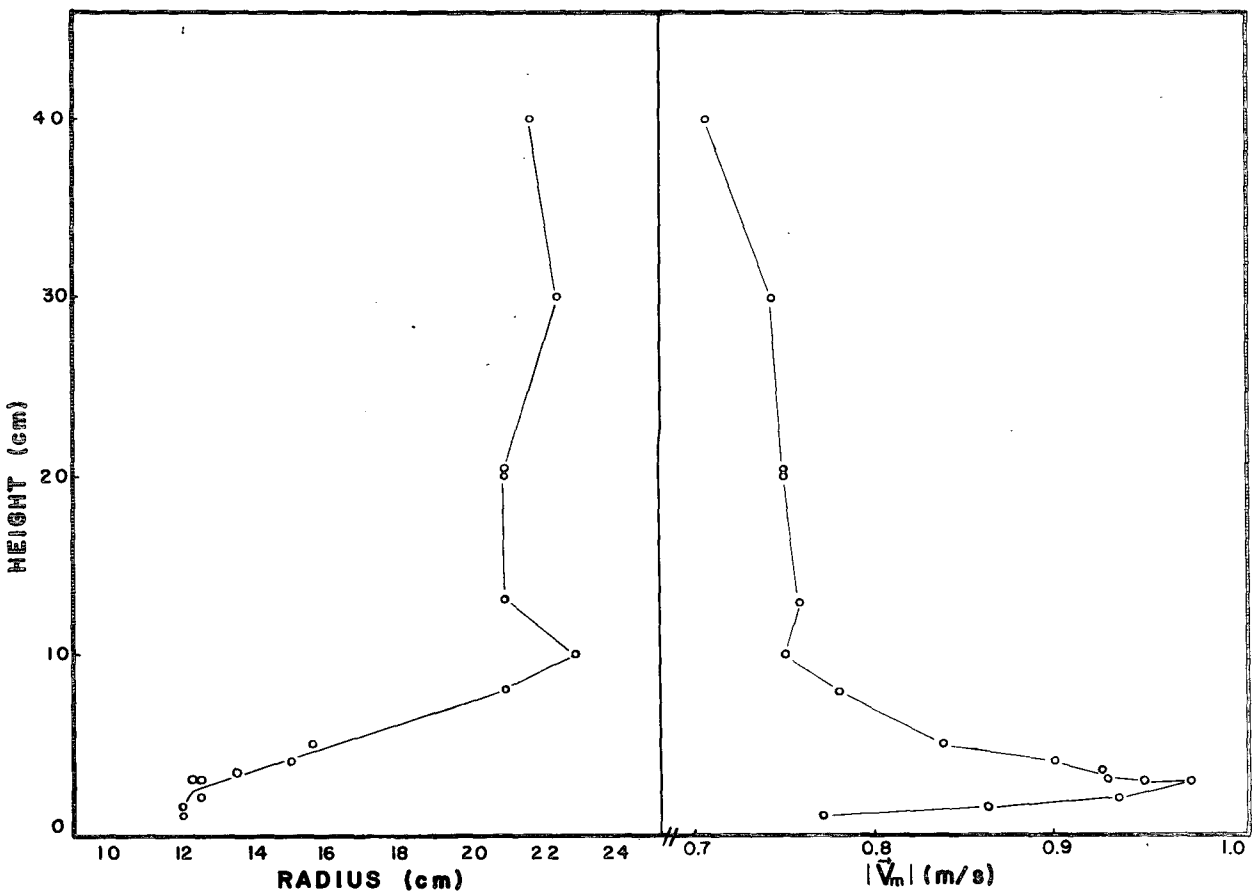

FIG. 4. A vertical scan of the time-averaged peak total velocity and the associated core radius for a typical turbulent vortex with a swirl ratio of 0.97 and a Reynolds number of 4.82×10^4.

The analysis of the core radius presented here applies to the region of a turbulent vortex core which is located well away from the direct influence of the lower rigid surface. By considering only an axisymmetric model, the complicating effect of the subsidiary vortices is removed. For the purposes of this analysis the vortex core radius is defined as the radius at which the tangential velocity is a maximum.

The time-averaged flow pattern is analyzed by dividing the flow into two distinct regimes and by examining the dynamic coupling between these regimes. The outer regime is characterized by the uniform convergence of inviscid swirling fluid. Here the effects of the surface boundary layer modification of the overall flow field may be disregarded for the large values of radial Reynolds numbers under consideration. Angular momentum is thus considered to be evenly distributed throughout the inflow layer so that the tangential velocity is dependent only on the radius and on the magnitude of the circulation. The time-averaged flow in the inner regime inside the vortex core is viewed as being governed by a balance between an axial pressure gradient force and the turbulent shear stresses within the core. The turbulent shear stresses arise as a consequence of the strong gradient in vertical velocity between the downward motion in the vortex core and the high-velocity updraft surrounding the core. The character of the inner flow regime may then be regarded as being very similar to that of turbulent flow in a rigid pipe in which an axial pressure gradient is balanced by a radial transport of axial momentum by turbulent eddies to the pipe wall with the principal effect of rotation being to dampen the turbulent velocity variations. Ward originally proposed the analogy of the vortex core flow with the "frictional flow in pipes" and stated that: "It appears that the pressure deficit at the base of a vortex core of sufficient length but of small diameter is maintained by these friction effects without local buoyancy or 'hydrostatic balance'." Applying this analogy to the case of the turbulent vortex, the "wall" of the pipe is then seen to be moving vertically upward with the velocity of the updraft surrounding the vortex. Even though the turbulent core fluid is rushing rapidly in the upstream direction with respect to the pipe wall, the velocity of the core fluid is small with respect to an observer at the fixed lower surface.

The vortex core may be viewed as representing a condition of dynamic equilibrium wherein opposing forces are in balance. Consider the effect of temporarily perturbing the core by increasing its radius slightly. Two processes act to restore the core to its original radius. First, the volume rate of flow (assumed to remain constant) is required to pass through a reduced annular region between the radii of the updraft opening and the vortex core, so that the average vertical velocity outside the core is thereby increased. For core radii >0.577 of the updraft radius the consequent increase in shear stress $\kappa(\partial w/\partial r)$, where κ is the eddy viscosity in the vicinity of the core wall, results in a net transport of core fluid in the positive z direction so that, by continuity, a decrease in the core radius results. Second, an increase in core radius causes a decrease in core pressure deficit since the pressure at the core radius due to the tangential velocity component is

$$\Delta P = \rho \frac{v^2}{2} = \frac{\rho \Gamma^2}{8\pi^2 r_1^2}, \tag{6}$$

where Γ is the constant value of the circulation outside the core and r_1 is the core radius. Since the tangential velocity vanishes at the downstream baffle, an estimate of the axial pressure gradient is given by

$$\frac{\Delta P}{Z} = \frac{\rho \Gamma^2}{8\pi^2 r_1^2 Z}, \tag{7}$$

where Z is the depth of the convective chamber above the inflow layer. Thus, other things being equal, a small increase in the vortex core radius causes a relatively large decrease in the axial pressure gradient. Since it is the axial pressure gradient that opposes the upward transport of core fluid by the strong shearing stresses within the core wall, a decrease in axial pressure gradient results in a net downstream (upward) flux of vortex core fluid. This process persists until the vortex core is returned to its original radius. These two mechanisms are not generally of equal importance. Specifically, for small cores, the radius is governed primarily by the variation in the axial pressure gradient, while for large cores it is governed by the variation in the axial shear stress.

By making the following simplifying assumptions regarding the time-averaged flow field in the inner and outer regimes, a unique relationship between the nondimensional core radius and the swirl ratio may be obtained:

(i) OUTER REGIME

$$u = \frac{-k}{r}, \qquad r > r_0 \tag{8}$$

$$v_1 = \frac{b}{r}, \qquad r > r_1 \tag{9}$$

$$w = 2a_1 h, \quad r_1 < r \leq r_0, \quad z < h. \tag{10}$$

The constants k, b and a_1 are determined by the radial Reynolds number, the circulation and the aspect ratio respectively.

(ii) INNER REGIME

$$u = 0, \qquad r \leq r_1 \tag{11}$$

$$v_2 = c(r - r'), \quad r' \leq r \leq r_1 \tag{12}$$

$$v_3 = 0, \qquad r < r' \tag{13}$$

$$w = w_i, \qquad r < r'. \tag{14}$$

The velocity profiles assumed here (shown in Figs. 5 and 6) are characteristic of a wide variety of two-celled turbulent vortex cores observed in the tornado simulator. Preliminary hot-film measurements of the individual velocity components recently completed for several swirl ratio values clearly demonstrate the essential features of these assumed profiles.

(iii) BOUNDARY CONDITIONS

(a) The vortex core radius is independent of z.
(b) The radial velocity at the core wall is zero.
(c) The vertical velocity at the ground plane is zero.
(d) The tangential velocity at the decoupling baffle is zero.

In the outer regime the Navier-Stokes equations and the equation of continuity for axisymmetric, incompressible, steady flow become

$$u\frac{\partial u}{\partial r} - \frac{v^2}{r} + w\frac{\partial u}{\partial z} = -\frac{1}{\rho}\frac{\partial p}{\partial r}, \tag{15}$$

$$u\frac{\partial v}{\partial r} + \frac{uv}{r} + w\frac{\partial v}{\partial z} = 0, \tag{16}$$

$$u\frac{\partial w}{\partial r} + w\frac{\partial w}{\partial z} = \frac{-1}{\rho}\frac{\partial p}{\partial z}, \tag{17}$$

$$\frac{\partial u}{\partial r} + \frac{u}{r} + \frac{\partial w}{\partial z} = 0. \tag{18}$$

The radial velocity in the updraft region may be found from Eqs. (10) and (18), i.e.,

$$u = -a_1 r\left[1 - \left(\frac{r_1}{r}\right)^2\right], \quad r_1 \leq r \leq r_0. \tag{19}$$

The total core pressure deficit at $r = r_1, z = h$ is now found by integration of Eqs. (15) and (17) from $r = \infty$ and $z = 0$, respectively, to be

$$\Delta P(r_1,h) = \rho\left[\beta\left(\frac{b}{r_1}\right)^2 + 2a_1^2h^2\right], \tag{20}$$

where

$$\beta = 1 - \frac{r'}{\gamma}\left(1 + \frac{r'}{\gamma}\ln\frac{r'}{r_1}\right). \tag{21}$$

Here β ranges from 0.5 to 1.0 as the width γ of the shear zone varies from 0.0 to r_1. Hence, β de-

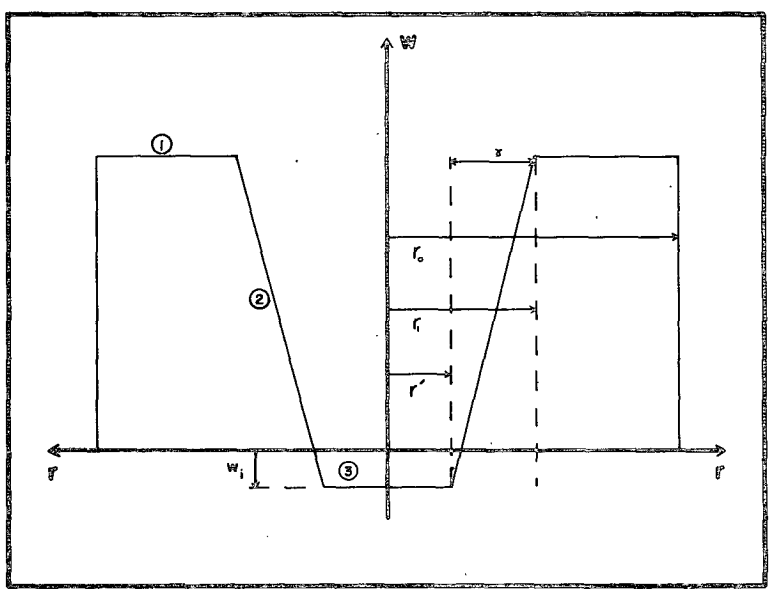

FIG. 5. Schematic of the idealized vertical flow field of a turbulent core (two-cell) vortex as used in the present analysis. Region 1 represents the relatively uniform vertical velocity between the edge of the updraft, r_0, and the radius r_1 of peak total core velocity. Region 2 is the thin layer of width γ, characterized by strong shear stresses, while region 3 is a relatively stagnant although turbulent central core of radius r' which has a small downward component w_i.

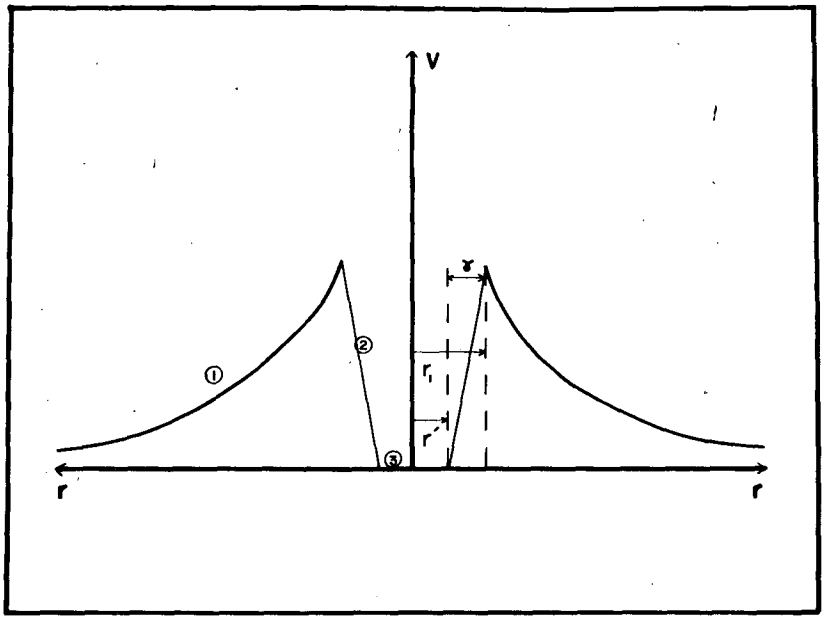

FIG. 6. Schematic of the idealized tangential flow field as used in the analysis. Region 1 represents the outer potential flow region in which angular momentum is conserved. Region 2, which lies between the radius r_1 of peak total velocity and the radius r' of zero tangential velocity is characterized by strong shear stresses through its width γ. Region 3 contains no tangential component since it arises from axially reversed flow of downstream air.

scribes the departure of the axial pressure deficit from that expected for a Rankine combined vortex in which $\gamma = r_1$ and $\beta = 1$. The average axial pressure gradient from $z = h$ to $z = Z + h$ is then

$$\frac{\Delta P(r',h)}{Z} = \frac{\rho}{Z}\left[\beta\left(\frac{b}{r_1}\right)^2 + 2a_1{}^2h^2\right]. \quad (22)$$

The balance of forces for the turbulent flow through a duct of diameter D may be written (see Schlichting, 1968)

$$\frac{\Delta P}{Z} = \frac{\lambda \rho W^2}{2D}, \quad (23)$$

where W is the mean axial velocity and λ the nondimensional coefficient of resistance.

Combination of Eqs. (22) and (23) eliminates the axial pressure gradient. The constants a_1 and b may be written as

$$a_1 = \frac{Q}{2\pi r_0{}^2}, \quad (24)$$

$$b = \frac{SQh}{\pi r_0}, \quad (25)$$

while W is approximated by

$$W = w - w_i. \quad (26)$$

The vertical velocity w in the annulus outside the core is

$$w = \frac{Qh}{\pi(r_0{}^2 - r_1{}^2)}. \quad (27)$$

The boundary condition that the radial velocity through the core wall is everywhere zero allows a continuity restriction to be placed on the flow inside the core in the form

$$M_i = M_0, \quad (28)$$

where M_i and M_0 are the mass fluxes into (downward) and out of (upward) the core respectively. For a thin shear layer M_i may be written

$$M_i \approx -\pi \rho r_1{}^2 w_i, \quad (29)$$

$$M_0 \approx \pi r_1 \gamma w \rho. \quad (30)$$

Solving for w_i gives

$$w_i = \frac{-\gamma w}{r_1}. \quad (31)$$

Eqs. (31), (26) and (27) may now be substituted into (22) and (23) with the expressions for a_1 and b to obtain a sixth-order polynomial for the vortex core radius dependence on swirl ratio:

$$r^{*6} + 2(S^2\beta - 1)r^{*4} - (4S^2\beta - 1)r^{*2} - \tfrac{1}{2}\lambda Z^* r^*(2\gamma^* + 1) + 2S^2\beta = 0. \quad (32)$$

Here r^* is the nondimensional core radius r_1/r_0,

$\gamma^* = \gamma/r_1$ is the nondimensional width of the shear layer and $Z^* = Z/r_0$ is a nondimensional convective depth aspect ratio. Terms on the order of w_i^2 have been neglected when compared with w^2. Eq. (32) may be inverted to obtain a more compact form for $S(r^*)$, i.e.,

$$\frac{r^*}{2\beta}\left[\frac{\lambda z^*(2\gamma^* + 1)}{2(r^{*2} - 1)^2} - r^*\right]. \tag{33}$$

Fig. 2 shows that Eq. (33) is in very reasonable agreement with the experimental data over a wide range in swirl ratios when a value of λZ^* of ~5 is chosen. The core radius is not well predicted for S values near zero, however. It should be pointed out that Eq. (33) shows the core radius to be independent of the aspect ratio as has been experimentally observed (Davies-Jones 1973).

If terms on the order of r^{*2} or less are neglected, Eq. (33) becomes

$$r^* = \frac{1.78S^2}{\lambda Z^*} \quad \text{for small } r^*, \tag{34}$$

where a value of γ^* of 0.1 has been chosen to simplify the expression. Thus the core radius shows a quadratic dependence on swirl ratio in this region.

b. *The maximum core velocity*

The interesting relationship represented by the peak velocity curve shown in Fig. 3 has not as yet completely yielded to any quantitative analysis. If an attempt is made to apply a simple Rankine-combined vortex model to this problem with the data of Fig. 2 supplying the appropriate value of the core radius and with the peak velocity given by

$$|\mathbf{V}_m| = (v^2 + w^2)^{1/2}, \tag{35}$$

a theoretical function may be found which agrees well with the data for swirl ratios ≥ 1.8. The Rankine-combined vortex model, however, predicts a singularity in $|\mathbf{V}_m|$ at $S = 0$ since the core radius goes to zero in this case. This is in conflict with experiment, which indicates that $|\mathbf{V}_m|/\bar{w}$ approaches a small finite value of ~0.5 at small S. (The value of 0.5 is expected from the potential flow solution for the non-swirling case at $z = h/2$.) It should be possible to develop a solution for very small S values by a perturbation technique. This still leaves the measurements for the most interesting range of S unexplained.

5. Conclusions and discussion

Ward made core radius measurements on single turbulent vortices for swirl ratios up to 0.55. The present data in Fig. 2 indicate that a considerably smaller core radius is obtained when measurements of the maximum total velocity are compared with the radius of the smoke-filled core measured by Ward. By electronically averaging the transient velocity variations in the multiple-vortex core structures which exist at higher swirl ratios, Ward's work has been extended up to a swirl ratio of 6. The nondimensional core radius r^* has been found to increase steadily with increasing swirl ratio, but to become progressively less dependent on S as S becomes large.

The r^* vs S curve contains data obtained for three radial Reynolds numbers: 5.76×10^4, 9.52×10^4 and 1.52×10^5. Since all three data sets lie on a single curve, it may be concluded that the core radius is not sensitive to the value of the Reynolds number over the range examined. This supports Ward's core radius results in which a variety of unspecified Reynolds numbers were used. Davies-Jones (1973) showed also that the nondimensional core radius was independent of aspect ratio when plotted against S. It is interesting that of the three independent parameters listed by Lewellen for vortex chamber flow, r^* appears to be insensitive to two—the radial Reynolds number and the aspect ratio.

By balancing the stress-induced upward vertical mass flux with the pressure-gradient-induced downward mass flux and by neglecting the mass flux through the vortex core walls and through the lower surface boundary layer, a simple expression for the nondimensional core radius as a function of swirl ratio may be deduced [Eq. (33)]. This expression predicts that the core radius is proportional to the square of the swirl ratio for small values of r^* and that r^* approaches unity in the limit of infinite S. This result is to be compared with the theoretical curves given by Ward (1972): $r^* = \sin^2\theta/(1 - K \times \sin^2\theta)$; and by Jischke and Parang (1974): $r^* = \tan^2\theta/(1 + 2\epsilon)$, where k and ϵ were taken to be much less than 1. By substituting $\tan\theta/2a$ for S in Eq. (34), the present analysis shows a similar r^* vs θ relationship for small S. Moreover, the present analysis also agrees well with experiment for very large values of S.

The expression for the core radius given in Eq. (33) involves two undetermined parameters: the dimensionless shear width γ^* and the coefficient of resistance λ. The value of γ^* must lie between the limits of 0 and 1. Analysis shows that the characteristic shape of the r^* vs S curve is only very slightly affected over this range of γ^*.[1] Thus, the form of the r^* vs S curve is essentially fixed and the parameter λ governs only the rate of increase in r^* with S. The magnitude of λ most closely approximating the experimental points was found to be near 1.9 which is substantially larger than values of λ commonly associated with turbulent flow through rigid pipes. In the

[1] So (1967) and Church (unpublished) have measured the vertical and tangential velocity profiles in the turbulent cores of vortices. Their results show that the value of γ^* varies over a relatively wide range for different swirl ratios.

case of vortex core flow, the magnitude of the turbulent eddies is not constrained by rigid boundaries to vanish at the vortex walls so that a much greater resistance to the axial flow is to be expected.

As pointed out by Davies-Jones (1973), the application of the Buckingham π-theorem yields six independent nondimensional parameters which uniquely describe the flow in the Ward type tornado chamber. The three most important parameters in modeling tornado-like flows are the radial Reynolds number, the swirl ratio and the aspect ratio. The remaining parameters are geometric length ratios, r_0/r_s, r_w/r_s and Z/r_s, where r_w is the radius of the convective chamber, r_s the radius of the rotating screen and Z the depth of the convective chamber. The Buckingham π theorem allows any three independent combinations of the four parameters r_0, r_s, r_w and Z to be chosen so that the alternate set r_w/r_0, Z/r_0 and r_s/r_0 is equally valid. The appearance of $Z^* = Z/r_0$ in the expression for r^* in (32) indicates that the importance of this "convective aspect ratio" should not be overlooked when attempting to model the dynamics of tornadic vortices. A typical value of Z^* for a tornadic storm may be estimated by taking values of Z and r_0 as ranging from 5–15 km and 1–3 km, respectively, so that Z^* ranges from 1.67–15. Values of Z^* for the Purdue chamber range from 1.04 to 6.25 depending on the value for r_0 and are thus geometrically similar in this respect to naturally occurring vortices. In comparing Ward's r^* versus S data with the present results it is seen that they lie consistently to the right of Ward's data in the region where there is duplication. Although other factors may have a bearing on this, a known difference in the two sets of experimental conditions is in the value of Z^*. For Ward's experiment Z^* was 1.50, while for the present work Z^* was 2.58. From Eq. (34) the pipe flow model predicts a decrease in r^* for an increase in Z^* from 1.50 to 2.58 which is in agreement with the observed trend.

The particular value of Z^* should not be of great importance in determining the core radius if 1) the vortex becomes disorganized by the action of turbulence before reaching the downstream boundary condition or 2) the core radius is much less than the total updraft radius along the full length of the vortex.

A final point concerning the result expressed in Eq. (33) is that the nondimensional core radius is predicted to be independent of the particular value of the aspect ratio employed. Although only one aspect ratio, 0.67, was used in obtaining the present data, Ward's data for a variety of aspect ratios was found to fit a single curve of r^* versus S as shown by Davies-Jones and was thus concluded to be independent of a.

In modeling the core radius dynamics the contribution to the vortex core mass flux due to boundary-layer convergence was assumed to be negligible. As a consequence of this, a central downdraft is predicted by the model for all values of swirl ratio. Since a central downdraft is not observed for small values of S (see Faler and Leibovich, 1978), the consequences of neglecting the boundary layer convergence should be examined. It is suggested that the direction of the vortex core flow is not as important as the magnitude of the vertical velocity gradient across the core wall in determining the core radius. This may be seen by computing the quantity $\partial r^*/\partial w_i$ which leads to the result that ∂r^* is proportional to $\partial w_i/w$ for small S, i.e., the change in core radius due to a change in the central axial velocity is small since w_i is much less than w. The pipe flow model results are therefore expected to be useful even for small swirl ratio values for which a central downdraft may not be present. The pipe flow model is not expected to be directly applicable to the very low S value domain for which the flow is essentially laminar.

Measurements of the time-averaged value of the nondimensional peak total velocities presented in Fig. 3 show that the peak velocity is an increasing function of swirl ratio for low values of S. For intermediate S values (0.4–2) the velocity is relatively constant, and for higher S values the velocity again increases smoothly. The data fit a single nondimensional curve quite well, and therefore indicate that the peak vortex velocity is directly proportional to the mean updraft velocity. It is also seen that the nondimensional peak velocity is relatively constant over a wide range of swirl ratios; i.e., for swirl ratio values from 0.4 to 2.4, $|\mathbf{V}_m|/\bar{w}$ lies between 2.4 and 2.8.

Given that the model tornadic vortices are dynamically and geometrically similar to those in nature, nondimensional physical quantities measured in the laboratory vortices should be representative of the corresponding quantities in actual tornadoes. It may therefore be expected that for a tornado which forms within the strong convective updraft of a mature cumulonimbus, the mean peak velocities in the core region well away from the surface will be about 2.6 times higher than the mean updraft velocity. Such a result should not, however, be directly applied to the winds near the surface because the dynamics of the vortex are strongly modified in this region by the boundary layer. The experimental results presented in Fig. 4 show that the highest velocities in the vortex occur close to the surface, with peak values which are some 30% higher than those measured well above the surface. The magnitude of this increase, in general, will depend on a number of factors, including the characteristic surface roughness length and the swirl ratio. Some experimental work has been reported on the effect of surface roughness elements on vortex

core velocities and radii, see Dessens (1972) and Leslie (1977).

It should be emphasized that the data presented in Fig. 3 do not represent the instantaneous peak velocities which occur in systems containing multiple vortices because these have been averaged out in the filtering process. As the velocity sensor encounters each rotating subsidiary vortex, its instantaneous response will be the resultant of the mean flow combined with that of the subsidiary vortex. The instantaneous peak velocity may be very different from the mean value. Leslie (1977) has measured the total velocity associated with a system containing four subsidiary vortices ($S = 3.18$) and has shown that the instantaneous peak values were about 85% higher than the mean for that particular system. Thus, even though the data in Fig. 3 do not indicate this effect, the higher swirl ratio vortex has a potentially much more damaging effect if multiple vortices are present.

Radiosonde measurements taken in severe storm environments (Davies-Jones, 1974) indicate that updraft velocities in excess of 35 m s^{-1} may be attained in tornadic storms. If the structure of the tornado may be identified as being similar to one of the modes observed in the tornado simulator (see Church *et al.*, 1979), then the corresponding swirl ratio may be inferred from the limiting values for that particular vortex mode. The nondimensional total peak velocity may then be found by referring to Fig. 3, from which the time-averaged peak total velocity in the tornado well above the influence of the lower surface boundary layer may be estimated.

6. Summary

Measurements have been presented of vortex radii and average peak velocities in turbulent modeled vortices. These were obtained in a Ward-type simulator for varying degrees of swirl. The core radius measurements duplicate the earlier experimental work of Ward for small values of swirl ratio. The new core radius values are considerably less than those measured by Ward. This is apparently a consequence both of the difference in the nondimensional convective depth Z^* and of the difference in the definition of the core radius. The core radius measurements were extended to higher values of the swirl ratio, for which no previous experimental data were available. The nondimensional core radius approached a value of unity in the limit of high swirl ratio. A dynamic model of the turbulent vortex core was developed from the Navier-Stokes equations where flow in the turbulent core was considered to be analogous to the turbulent flow in a pipe, and a dynamic balance was established between the wall shear stress and the axial pressure gradient force. This resulted in a relation for the core radius as a function of the swirl ratio, a coefficient of resistance λ and a dimensionless shear width γ^*. By choosing an appropriate value of λ, a curve of the function $r^*(S)$ was drawn which gave a good fit to the experimental data. (The result was found to be only weakly affected by the value of γ^*.) For small S values this function reduced to a form which agreed well with the general results developed by Ward and by Jischke and Parang, in spite of being derived from a completely different physical viewpoint.

Measurements of the averaged values of the peak velocity in turbulent cores identify the mean updraft velocity as the principal scaling parameter for the mean total core velocity. It was also noted that the time-averaged peak velocity values were not strong functions of the swirl ratio. The nondimensional velocity values are considered valid for certain regions in single turbulent tornadoes, although they must be applied with caution elsewhere. A vertical scan of peak velocities showed that the highest values occurred close to the surface. In order to obtain a more complete appreciation of the complexities of vortex flows further experiments are required. In particular, future experiments should focus on a systematic examination of the influence of surface roughness elements on core dynamics, on the structure of the three-dimensional boundary layer associated with the vortex flow, and on a determination of the separate components of velocity associated with the various vortex types.

Acknowledgements. The authors would like to extend thanks to their colleagues Drs. E. M. Agee and J. T. Snow and Mr. H. Niino for useful discussion of various aspects of this work, to Miss B. J. Barnhart for assistance in obtaining the results presented here, and to Miss V. Ewing for the typing of this manuscript. This research was supported by the Atmospheric Science Section, National Science Foundation under Grant ATM 77-16955.

REFERENCES

Church, C. R., J. T. Snow and E. M. Agee, 1977: Tornado vortex simulation at Purdue University. *Bull. Amer. Meteor. Soc.*, **58**, 900–908.

——, ——, G. L. Baker and E. M. Agee, 1979: Characteristics of tornado-like vortices as a function of swirl ratio: a laboratory investigation. *J. Atmos. Sci.*, **36**, 1755–1776.

Davies-Jones, R. P., 1973: The dependence of core radius on swirl ratio in a tornado simulator. *J. Atmos. Sci.*, **30**, 1427–1430.

——, 1974: Discussion of measurements inside high-speed thunderstorm updrafts. *J. Appl. Meteor.*, **13**, 710–717.

——, 1976: Laboratory simulations of tornadoes. *Proceedings of a Symposium on Tornadoes: Assessment of Knowledge and Implications for Man.* Texas Tech Univ., Lubbock, Texas 151–174. [Available from the Inst. for Disaster Research, Texas Tech. University, P.O. Box 4089, Lubbock].

Dessens, J., 1972: Influence of ground roughness on tornadoes: A laboratory simulation. *J. Appl. Meteor.*, **11**, 72–75.

Faler, J. H., and S. Leibovich, 1978: An experimental map of the internal structure of a vortex breakdown. Part II. *J. Fluid Mech.*, **86**, 313–335.

Jischke, M. C. and M. Parang, 1974: Properties of simulated tornado-like vortices. *J. Atmos. Sci.*, **31**, 506–512.

Leslie, F. W., 1977: Surface roughness effects on suction vortex formation: a laboratory simulation. *J. Atmos. Sci.*, **34**, 1022–1027.

Lewellen, W. S., 1962: A solution for three-dimensional vortex flows with strong circulation. *J. Fluid Mech.*, **14**, 420–432.

Schlichting, H., 1968: *Boundary Layer Theory*, 6th ed. McGraw Hill 748 pp.

So, K. L., 1967: Vortex phenomena in a conical diffuser. *AIAA J.*, **5**, 1072–1078.

Ward, N. B., 1972: The explanation of certain features of tornado dynamics using a laboratory model. *J. Atmos. Sci.*, **29**, 1194–1204.